Mapping out Local Field Enhancements of Surface Nanostructures

Division of Synchrotron Radiation Research
Lund University

B. Sc. Thesis
June 2013

LUND
UNIVERSITY

Author
Björn Erik Skovdal

Supervisor
Prof. Anders Mikkelsen

Abstract

Photoemission electron microscopy was used to study the optical properties of wurtzite InAs nanowires. Linearly polarized femtosecond laser pulses illuminated the sample of nanowires and generated photoelectrons through multiphoton photoemission. These electrons could then be detected to create an image. Several different nanowires have been investigated, but only straight, single nanowires have been measured upon. The intention of the measurements was mainly to study the photoemission from the nanowires as a result of changing the state of polarization in the illuminating laser light. To see if there was any relation between the angle of polarization and the orientation angle of the wire, a diagram with the angle of the polarization that generated the most photoelectrons against nanowire orientation angle was made. The diagram showed a strong relation between the two. These results were compared to the results from earlier experiments conducted in 2012.

Acknowledgements

I wish to thank Prof. Anders Mikkelsen for making this thesis possible and and PhD student Erik Mårsell for guiding me through it, answering all my questions and even lending me some of his books.

Additionally, I would like to thank prof. Anne L'Hullier at the Division of Atomic Physics for supplying the laser system, as well as PhD student Piotr Rudawski and Post Doc Miguel Miranda for tuning it for the purposes of this thesis.

I would also like to thank the group of Dr. Kimberly Dick Thelander for growing the nanowires that were investigated in this thesis.

Table of Contents

1 Introduction

The curious mind of mankind has led us to the advanced society we live in today. As the hunger for information failed to cease, the microscopic world of the very small was revealed to us through microscopes. But as we continued to advance towards the boundaries of the nanoscopic world, visible light was no longer sufficient to resolve the landscape of atoms and molecules. More advanced microscopes had to be developed, and today there are many different kinds of electron microscopes able to reveal the secrets of the nanoscopic realm.

Not only is it possible to investigate the nanoscopic world through microscopes; creating and manipulating nanoscale structures can be done in modern labs. It so happens that Lund Nano Lab produces world class nanowires.

The focus of this thesis was to study and map out field enhancements of surface nanostructures. This has been done by investigating the optical properties of Indium arsenide (InAs) nanowires, produced by Lund Nano Lab, using photoemission electron microscopy with a pulsed femtosecond laser at Lund Laser Centre. Exactly how these field enhancements in these nanostructures arise has not yet been fully understood.

2 Theory

2.1 PEEM-*Photoemission Electron Microscopy*

In a photoemission electron microscope electrons are emitted from a sample by means of photo-ionization. The emitted electrons then travel through electrostatic lenses to form a magnified image and thus, information of sample can be extracted through interactions with light. If structures on the sample do not emit electrons, they are effectively invisible. This can be the case if the illuminating light is not, at moderate intensities, energetic enough to knock out any electrons. A contrast in the images can thus be created by choosing the frequency of the illuminating light so that some structures emit electrons and some do not. The PEEM operates in ultra-high vacuum (UHV) to ensure that the electrons reach the detector on the other side of the PEEM without colliding with air molecules.

2.1.1 Light-Matter Interaction

As Richard Feynman simply explains in his book *QED - The Strange Theory of Light and Matter*, there are only three basic actions that involve photons and electrons, where the first two are the movements of photons and electrons. While the third is; an electron can emit or absorb a photon. The emission and absorption of a photon is fundamentally the same thing and the probability for an electron to emit or absorb a photon is the same. These three actions alone accounts for all phenomena involving light and electrons. [1]

When a photon comes in contact with matter, the photon has a certain probability to be absorbed by an atomic system. When the photon is absorbed all of its energy can be used to excite an electron to a higher energy state. The probability for this transition to happen depends on the photon energy relative to the energy difference between the two levels in the atom. The probability is highest when the photon energy coincides with the energy difference between the two energy levels, that is, when the detuning is zero. [2] See figure 2.1 below.

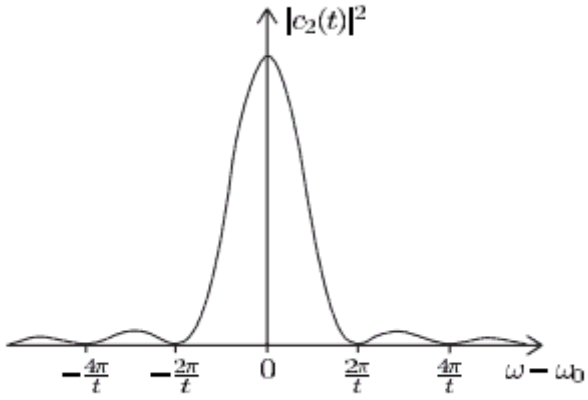

Figure 2.1 The probability of being in the excited state in a two level atom illuminated by monochromatic light as a function of the detuning. Image taken from Christopher J Foot, Atomic physics.

2.1.2 The Photoelectric Effect

If the photon energy is high enough it can expel the electron from the atom, i.e. ionizing it. This is what is called photoemission of an electron. Increasing the energy of the photon will increase the kinetic energy of the emitted electrons. The maximum kinetic energy of the electrons is determined by

$$\frac{1}{2}mv_{max}^2 = E_{photon} - \phi \quad (1)$$

where ϕ is the work function, the minimum energy needed to expel the electron from the atom. The valence electrons, which are the least tightly bound, outermost electrons, will be ejected with the maximum kinetic energy. [3] Inner electrons that are more tightly bound will be ejected with lower kinetic energy because the work function for them is larger. Note that according to equation (1) there should be no photoemission if the photon energy is lower than the work function.

2.1.3 MPPE -*Multiphoton Photoemission*

If the photon energy is lower than the work function, there is still a probability for photoemission to occur. This is because an electron can be momentarily excited to higher energy level by a photon, and then further excited by another. This process can continue any number of times until the electron is emitted and the atom is ionized. Even if the photon energy does not match the energy difference between two levels, the electron can still be excited to a so called virtual state, where from it can be further excited. Multiphoton photoemission requires high photon intensities as the lifetime of excited states are usually extremely short. If the photon intensity is too low, a second photon will simply not be on time to further excite the atom before it has decayed back into a lower state. Intensities high enough for MPPE to occur can be acquired with lasers. An atomic system can absorb photons even after it has been ionized. This can further increase the kinetic energy of the emitted electron with a multiple of the photon energy. This is called Above Threshold Ionization (ATI) and will not be further discussed since it is of little relevance.

2.1.4 Energy Levels in Solids

Light-matter interactions have so far only been considered for free atoms, and not solids. However, the most prominent difference between free atoms and solids is the structure of the energy levels. When an atom is brought close to another atom, to form a molecule for instance, the energy levels of the atoms are distorted, resulting in a quantum mechanical splitting of levels. If more atoms are brought close, the levels will split again and again etc. Eventually the energy levels will form bands that are considered to be quasi continuous, these bands can have gaps in between them, just as atoms have gaps in between their energy levels. The size of these gaps may define the type of solid. An insulator has the Fermi level located in between a large band gap, so that excitations over the gap require high energies. This is the fundamental reason for the low conductivity of insulators. The Fermi level is defined as the energy level for which there is a 50% probability to be occupied in thermodynamic equilibrium. Semi-conductors have smaller band gaps than insulators and metals

have no band gaps, overlapping bands or the Fermi level located in the middle of one of the bands. Therefore, excitations are easy, and as a result, metals are good conductors.

2.1.5 Charging

A sample that is constantly illuminated by ionizing light will become positively charged as electrons are emitted from the sample. This could cause distortion to the image and endanger damage to either the sample or the PEEM itself. This can be avoided by keeping the sample conducting and at ground potential at all times. [4]

2.2 PEEM Vacuum

The PEEM is operating in Ultra High Vacuum (UHV) because the distance electrons can travel in normal atmospheric pressure before they collide or are absorbed by molecules in the air is only in the order of microns and the length of the PEEM is roughly 2 meters. UHV then enables most of the electrons to travel through the entire length of the PEEM without interacting with air molecules.

2.2.1 Baking the Chamber

Water vapor and other gases condense on the inside of the chamber walls. This condensation cannot be removed by the pumps alone, even though the pressure in the chamber is significantly reduced. The chamber must be heated to roughly 100^{o}C for at least 24 hours. This procedure, also known as baking, ensures that most of the vapor evaporates from the chamber walls and thereafter are removed by the vacuum pumps. The chamber should be covered with Al-foil in order to supply increased and more even heat conduction. Baking is crucial if UHV is to be achieved.

2.2.2 Vacuum Pumps

One vacuum pump alone can never reach UHV because different types of pumps work in different regimes of pressure. Thus, in order to reach and maintain UHV, a conjunction of different types of vacuum pumps must be used. The different types of pumps that are used for evacuating the PEEM chamber are presented below.

2.2.3 Rotary Vane Pump

The rotary vane pump is an oil-sealed pump that works in the pressure range of 1 - 10^5 Pa. Figure 2.2 below shows the design of the pump.

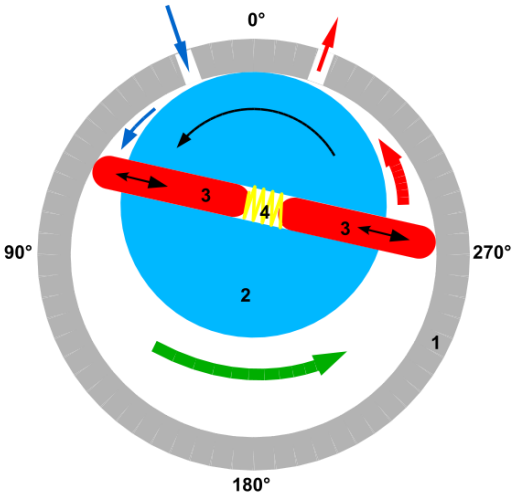

Figure 2.2 Schematic design of a rotary vane pump. 1, outer casing, 2 rotor, 3 vanes, 4 spring. The vacuum chamber to be evacuated would be positioned above the blue arrow. Figure taken from http://en.wikipedia.org/wiki/File:Rotary_vane_pump.svg, verified 2013-06-17. Author: Rainer Bielefeld

As figure 2.2 shows, the rotor is placed off-center with respect to the outer casing and a spring makes sure that the two vanes always are fully extended in order to make an air tight seal. A low vapor pressure fluid also helps to seal the vanes and the surfaces between the housing and the rotor, additionally, it works as lubricant. When the first vane passes by the inlet, air will be forced into the growing region because of the much higher pressure in the vacuum chamber to be evacuated. The air will continue to fill the compartment until the other vane passes by the inlet and seals off the region. When the first rotor passes by the outlet, air will be forced out through the outlet as the region diminishes and the air pressurizes. The outlet is oil-sealed in order not to allow any air back into the pump. [5]

2.2.4 Turbomolecular Pump

The turbomolecular pump transfers momentum to gas molecules by collisions with high-speed rotating blades. The maximum speed of a turbomolecular pump is roughly 80,000 rpm, which corresponds to velocity of 500 m/s on the tips of the blades. One single row of blades is not enough to reach UHV, turbomolecular pumps usually have between 8-20 discs of blades. A turbomolecular pump does not work in atmospheric pressure and therefore needs another vacuum pump, such as a rotary vane pump, to bring the pressure down to operational pressures. A pressure of 10^{-8} Pa is reachable with a turbomolecular pump and a baked vacuum chamber. The inside of a turbomolecular pump is shown in figure 2.3 below where all the different blades can be seen. [5]

Figure 2.3 Interior of a turbomolecular pump. All the layers of rotating blades can be seen. Figure taken from http://en.wikipedia.org/wiki/Turbomolecular_pump, verified 2013-06-17. Author: liquidat

2.2.5 Ion Pump

When high vacuum is reached, through the usage of different mechanical vacuum pumps, the pressure in the vacuum chamber can be maintained and even further decreased through the usage of ion pumps. An ion pump uses electric and magnetic fields to keep electrons circulating between an anode and a cathode for an extended period of time without reaching the anode. These electrons collide with, and thus, ionize air molecules in the chamber. Theses ions then feel the electric potential of approximately 5 kV and consequently stick to the cathode. As the ions collide with the cathode and other air molecules, secondary electrons are released that can enter the circular orbit to further ionize the gas. The electric and magnetic fields that prevent the electrons from reaching the anode is crucial, as it increases the distance the electrons travel before they collide, this enhances the probability of ionizing collisions. The steady state of about 10^{10} electrons/cm^3 in orbit is reached after nanoseconds for pressures at 10^{-1} Pa, while roughly 500 s at 10^{-9} Pa. [5]

2.3 Illumination and the Beam

2.3.1 Polarized Light

In order to describe light, at least three dimensions of space are needed as the wavevector **k** which points in the direction of propagation**,** the electric field vector **E** and the magnetic field vector **B** are all perpendicular to each other. The polarization of light describes how these three vectors are directed in space and typically there are four different types of polarization, unpolarized, linearly polarized, circularly polarized and elliptically polarized. The polarization can be described by decomposing **E** into two perpendicular vector components, when these vectors have the same amplitude and are in phase, the light will be linearly polarized, and **E** will oscillate in only one plane. However if the vector components are 90^o out of phase the light will be circularly polarized, **E** will then rotate around **k** with the same amplitude all the time. Elliptically polarized light is obtained

when either the amplitudes of the vector components differ from each other or if they are out of phase by anything but 90°. Unpolarized light implicates that the distribution of polarization is random amongst all photons. This means that a source of unpolarized light, such as the sun, emits photons with all types of polarization. However when measured, a single photon is either linearly, circularly or elliptically polarized, it can never be unpolarized. When the electric field of linearly polarized light oscillates in the plane of the sample, it is called s polarized and when it oscillates in the plane of incidence it is called p polarized. See figure 2.4 below.

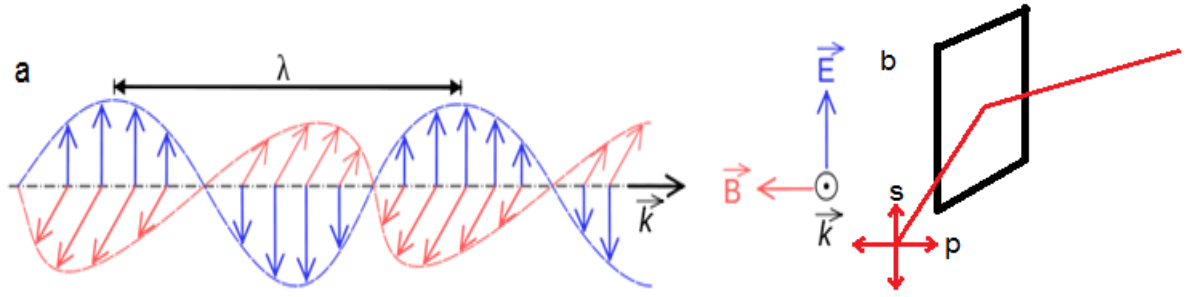

Figure 2.4 *a) A linearly polarized electromagnetic wave. The electric and magnetic fields oscillate perpendicular to each other at all times. The wavelength of the wave is indicated by λ. b) s- and p-polarized light incident on the surface of a sample. Image a) taken from:* http://en.wikipedia.org/wiki/File:Onde_electromagnetique.svg, verified 2013-06-17. Author SuperManu

2.3.2 Birefringence and Half Wave Plate

A birefringent crystal has a refractive index that depends on the state of polarization and direction of propagation of light. This anisotropy arises from the crystal structure of the material. A birefringent crystal has two orthagonal axes with different index of refraction, often called the slow and the fast axis. Linearly polarized light with **E** parallel to the fast axis will travel through the crystal faster than light with **E** parallel to the slow axis. If **E** is in between the two axes, the components of **E** will travel through the crystal at different speeds. In a half wave plate the thickness of the crystal is chosen such that the phase shift of the two components is half a wavelength, therefore a half wave plate only works for a specific, small bandwidth of wavelengths. This phase-shift results in a rotation of the electric field vector **E** by twice the angle that the crystal is rotated. If **E** is parallel to either the slow or the fast axis, the state of polarization will not be changed after the half wave plate.

2.3.3 Brewster Angle

When unpolarized light hits a glass plate, some light is reflected, and the amount depends on the thickness of the glass. [1] However, if the glass plate is inclined with respect to the incident light by an angle

$$\theta_B = \arctan\left(\frac{n_2}{n_1}\right) \tag{2}$$

where n_1 and n_2 are the index of refraction of the incident medium and the glass plate respectively, then p-polarized light will be transmitted with little losses and some of the s-polarized light will be reflected. $\theta_B$is called the Brewster angle and a glass plate at this angle is often called a Brewster

window. If a Brewster window is placed inside a laser cavity, a few percent of the s-polarized light will be lost in each passage through the inclined glass plate, both in the forward and backward direction. The gain for s-polarized light will thus be reduced while more or less unaffected for p-polarized light and effectively the output of the laser will be p-polarized.

2.4 Laser - *Light Amplification by Stimulated Emission of Radiation*

Since the first lasers in the 1950s we have come a long way of developing new, more advanced lasers. The research lasers of today can occupy entire rooms or even large facilities, pulsed lasers can reach pulses as short as a few hundreds of attoseconds and photon intensities as high as 2×10^{22} W/cm^2 has been reached. [6]

The field of application for lasers has proven to be enormous and today, lasers can be found virtually anywhere in the modern society. A few examples are in DVD-players, laser cutting and in medical applications. Lasers are also widely used in research. It is popular because it can provide coherent and monochromatic light with high photon intensities. These properties prove to be useful in many fields of scientific research. Although the linewidth of a laser can be extremely small, a completely monochromatic laser cannot exist due to Heisenberg's uncertainty principle, as discussed in section 2.4.5.

2.4.1 Principles of a Laser

A laser is based on the process of stimulated emission, which is a light-matter interaction that occurs when a photon passes an atom. An excited atom then interacts with the electromagnetic wave and de-excites to a lower energy level, the process creates an additional photon that is equal in every way to the incident photon that stimulated the process. (The additional photon has the same frequency, phase, polarization and direction as the incident photon.) This process requires that the incoming photon has the same energy (or roughly the same) as the energy difference between the two levels in the atom. However, if the atom is in the lower state, there will be no stimulated emission and the photon will be absorbed instead.

Since absorption leads to losses in photon intensities, the medium is pumped to ensure that the population of states is in the higher energy level and not in the lower, as it thermodynamically would want to. The pumping creates a so called population inversion. See figure 2.5 below. When the atoms are pumped to state 2, they will quickly relax down to state 3 where they further relax down to state 4, preferably through stimulated emission. Upon reaching state 4, the atoms will quickly relax down to the ground state, where they will be quickly pumped back up to state 2 again, provided that the pumping is sufficient. [7] The intention is to have a large population at all times in level 3 (hence the longer lifetime), and a low population in the other levels, especially level 4. This is because, as the atoms populated in level 3 contribute to stimulated emission, and thus lasing, the atoms in state 4 prevent lasing by absorbing photons. An atom has a probability to relax directly from state 2 to state 1 or 4 without passing by state 3, however all these "wrong" transitions are less probable than the "right ones" in a well-functioning laser. There are lasers that employ 3-level diagrams as well where the ground state acts as the lower lasing level, however, 4-level lasers are superior to 3-level lasers. [7]

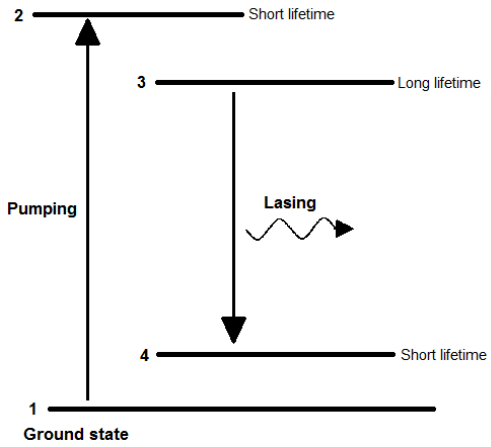

Figure 2.5 Energy level diagram of a 4-level laser. The lifetime of level 3 can be in the microsecond regime while the lifetime of level 4 can be as short as picosecond.

2.4.2 Laser Pumping

Laser pumping can be done in a variety of ways, both electrical and optical pumping are commonly used techniques. Flashlight pumping is an optical pumping technique where the lasing medium is encircled with or next to a lamp that is tuned to excite the atoms in the lasing medium from level 1 to 2. Another pumping technique, often employed by gas lasers, uses a direct current of electrons between an anode and a cathode placed at each end of the lasing medium. The electrons will collide with gas molecules as they travel from the cathode to the anode and thus excite the atoms. A common technique is to pump lasers with other lasers, external laser pumping. The pumping laser can be a diode laser or any other type of laser. For maximum efficiency, the wavelength of the pump laser should be on resonance with the energy difference between level 1 and 2 in the laser that is to be pumped. [7]

2.4.3 The Laser Cavity

The lasing medium is placed inside a laser cavity that consists of two mirrors, this makes the photons bounce back and forth through the lasing medium which permits more stimulated emission. One of the mirrors is semi-transparent. This allows the beam to actually escape the cavity.

Due to interference, standing waves of light will arise inside the laser cavity. These different modes, as they are often called, depend both on the cavity parameters and the gain medium (lasing medium). The cavity itself can support a large number of longitudinal modes since the wavelength of light is usually much shorter than the length of the cavity. However the gain medium does not support such a broad spectrum and thus the frequencies that are lasing are the ones that are supported by both the cavity and the lasing medium simultaneously.

2.4.4 Mode Locking

The different longitudinal modes normally oscillate independently in a continuous wave laser, though there are techniques to lock their phases together in order to obtain ultra-short laser pulses such as femtosecond pulses. There are active and passive ways to accomplish these so called mode locking techniques. In active mode locking, an optical switch that is controlled externally is placed inside the laser cavity. The switch is only opened at short periods of time when the pulses are supposed to pass

through. At all other times, the switch blocks the light. Thus, the prevailing pulses are unaffected by the switch and any light with a different phase will be quenched as it suffer from too great losses. Thus, mode locking can be said to happen by accident, when the phases of different modes happens to employ equal values and are allowed to pass through the optical switch they continue to be locked, but until this happens, no lasing can occur. Passive mode locking works under the same principle, however instead of having an active switch, a saturable absorber or a Kerr-lens is placed inside the laser cavity. The transmission coefficient of a saturable absorber increases as the light intensity passing through it increases. Consequently it lets high intensity pulses through but blocks out the weak ones. This automatically forces the system to mode lock without any controllable switch since lasing can only occur if the phases of the modes are locked and create high intensity pulses. A Kerr-lens is made out of a material that through nonlinear-optical phenomena focuses high intensity light to a greater extent than low intensity light. Thus, the high intensity light can be let through a small aperture that blocks out the, less focused, low intensity light. [7]

2.4.5 Heisenberg's Uncertainty Principle in Pulsed Lasers

As mode locking generates ultra-short pulses, the frequency range must be increased. This has nothing to do with the mode locking technique itself, but is a fundamental property of nature, a consequence of Heisenberg's uncertainty principle. Heisenberg's uncertainty principle limits the maximum precision of two simultaneously measured variables, corresponding to two non-commuting operators. The energy-time uncertainty is given by

$$\Delta E \Delta t \geq \frac{\hbar}{2} \tag{3}$$

where $\hbar$ is Planck's constant divided by 2π, ΔE is the standard deviation in energy and Δt is the average amount of time it takes for an arbitrary operators expectation value to change by its standard deviation. There exists no Hermitian time operator in quantum mechanics. For photons, the energy is related to the frequency in the following way

$$E = \hbar\omega \tag{4}$$

where ω is the angular frequency of the photon. This yield

$$\Delta\omega \Delta t \geq \frac{1}{2} \tag{5}$$

where, for pulsed signals, $\Delta\omega$ and Δt are the spectral and temporal root-mean-square widths of the pulse respectively. [8] Equation (5) is called the time-bandwidth product and is the fundamental limit to any type of pulsed signal. For a Gaussian pulse, with $\Delta\nu$ and Δt defined as the full width half maximum (FWHM) of the pulse, the minimum value of the time-bandwidth product is

$$\Delta\nu \, \Delta t \approx 0.44 \tag{6}$$

this can be shown using the Fourier theorem. [9] Note that the frequency ν is used in equation (6) as opposed to the angular frequency ω in equation (5).

This explains why a laser can never be completely monochromatic. The shorter the laser pulse, the larger the linewidth must be. Thus, to produce femtosecond pulses the lasing medium must have a

linewidth in the THz regime. For example, a Titanium-doped sapphire laser has a linewidth of 100 THz and pulse duration of 10 fs. [7]

2.5 Additional Microscopes

Although the PEEM was the primarily used microscope in this thesis, two other types of microscopes were used as complimentary microscopes. This section will briefly discuss these two microscopes

2.5.1 Optical Microscopy

Optical microscopy uses visible light to illuminate a sample and optical lenses to magnify the image. The resolution of such a microscope is often limited by the fact that the human eye is used as the detector. The resolution is therefore fundamentally limited to roughly 400 - 700 nm.

2.5.2 SEM - *Scanning Electron Microscopy*

The SEM uses a focused electron beam to scan over a sample. These electrons can back-scatter on the surface of the sample or interact with it to produce secondary electrons that can be detected. The image of the sample is then created by the detected signal and the position of the electron beam. The resolution of any instrument or microscope is fundamentally limited by the wavelength of the particles that carries the information as explained in section 3.4, and since the wavelength of the electrons are usually much shorter than the wavelength of visible light, the lateral resolution of the SEM is generally much better than that of an optical microscope. The de Broglie wavelength of the electrons are inversely proportional the velocity of the electrons, thus the wavelength can be varied by tuning the acceleration voltages.

The SEM has a different contrast than a PEEM, and contrary to PEEM the physical structure of the sample is resolved, and not the optical properties. Because of this and its high lateral resolution, SEM is a great complimentary technique to PEEM.

Since the sample is bombarded with electrons, it is crucial to have a well conducting sample, thus to efficiently abduct electrons from it. Otherwise charging effects will occur and distort the image. Too violent charging effects can even destroy the sample completely.

3 Method

This section presents the experiments that were made and all the preparations involved.

3.1 The Samples

3.1.1 Nanowire Growth Method

The nanowires were grown in the Lund Nano-lab by the group of Kimberly Dick Thelander using the Vapor-liquid-solid (VLS) nanowire growth method realized in a Metal-Organic Vapor Phase Epitaxy (MOVPE) chamber. This is done by placing Au particles on an InAs(111)B substrate surface which is then placed in the chamber and heated. Thereafter Tri-methyl-indium (TMI) and arsine (AsH_3) gas are let into the chamber. The TMI molecules are chemically decomposed so that a supersaturated alloy of Au and In is created, the In atoms then crystallizes under the Au particle and the nanowire grows upwards with the Au particle on top of the wire. The As atoms reach the interface between Au particle and nanowire through surface diffusion after they have been adsorbed on the surface of the wafer. The temperature is regulated to catalyze nanowire growth under the Au particle, but to avoid bulk growth. [10,11]

3.1.2 Samples and substrates

When the nanowires had grown they were transferred to the sample substrate by simply scratching them off with a piece of paper, and then carefully stroking them onto the sample substrate; this has been given the fancy name *The Dry Deposition Method*. Using a metallic film on a semiconductor substrate reduces problems with charging.

The samples were:

Sample 1: Wurtzite InAs (with stacking faults), on a 55 nm thick Cr-film on Si(111) substrate

Sample 2: High purity wurtzite InAs , on a 55 nm thick Cr-film on Si(111) substrate

The energy needed to knock out an electron in an InAs nanowire is only roughly known, though it is probably close to 4 eV. A laser of 800 nm (1.54 eV) then requires 3 or 4 photons to release one electron.

3.1.3 Preparations

The first sample was placed in a PEEM sample holder and an optical microscope was used to make sure it was placed flat in the sample holder and not tilted. This was done by looking for focus changes at the edges of the sample. It is crucial that the sample is lying flat on the sample holder as the sample is approximated as an infinitely large, flat, perfect conductor in the PEEM. If the sample is slightly tilted, the field near the sample will be slightly asymmetric. This leads to astigmatism, which negatively affects the resolution and distorts the image. It also makes it harder to optimize the setting of the microscope, and each time the sample is moved, the setting must be re-adjusted. When the sample was successfully placed in the sample holder, the sample was ready to be investigated in the PEEM.

3.2 The Experiment

3.2.1 Execution

The sample was placed in a small, separate vacuum chamber that was pumped using a rough pre-pump and a turbo pump. When the pressure was sufficiently low, the sample was inserted in the PEEM through the PEEM's transfer-system. The sample was initially studied with the PEEM in UHV using the Hg-lamp that is presented in section 3.5.1. This was done in order to get an overview of the sample with the intention of finding interesting nanowires. When interesting areas were found, the Hg-lamp was switched off and the laser beam was directed onto the sample. The polarization of the beam was changed from 0^o to 360^o with increments of 10^o, where images were taken. The polarization angle was altered with a broadband half wave plate that supported wavelengths from 690 to 1200 nm. A broadband half wave plate is necessary since the laser beam is quite broadband. The images were recorded using two different CCD cameras that are presented in section 3.3.4 below.

3.2.2 A Burned Power Supply

The intention was to additionally study high purity wurtzite InAs nanowires (sample 2), and to compare the results with the less pure wurtzite InAs nanowires (sample 1). After enough data had been collected from sample 1, sample 2 was inserted in the PEEM and investigated with the Hg-lamp. An extensive map of plenty of good looking wires was made, but unfortunately the laser was not working properly at the time. The week after that, when the laser was working, another effort to further investigate the wires with the laser was made. However, only moments after the PEEM was turned on, the electronics of the PEEM began to give out smoke. The power supply of the PEEM was damaged and had to be sent to the manufacturer. This prevented further investigation of sample 2 and thus, only data from sample 1 has been analyzed.

3.3 The PEEM

3.3.1 Focus IS-PEEM

The photoemission electron microscope was a FOCUS PEEM with Integral Sample Stage (IS-PEEM) from Omicron nanotechnology GmbH. The PEEM has an integral, piezoelectrically driven, sample stage. The sample can only be moved in the plane of the sample itself. The sample stage is in unit with the objective to attenuate any relative motion between the sample and the objective. This results in less vibration compared to having a separately mounted sample stage. The sample stage is enclosed in μ-metal shielding in order to protect against disturbing magnetic fields. [12] The PEEM has a transfer-arm with a separate vacuum chamber which allows for changing of samples without venting the main chamber. There are also windows around the sample stage so light can reach the sample. These windows are positioned such that the incoming light can enter at a maximum grazing angle of roughly 30^o. [12] The laser beam comes in at a grazing angle of 25^o.

3.3.2 Electrostatic Lenses

The PEEM is equipped with an extractor positioned right in front of the sample. The sample was at ground potential at all times, while the potential difference between the sample and the extractor was altered between 10-13 kV in the experiments. The sample and the extractor, as well as the focus

and the column electrode form the electrostatic tetrode objective lens. There is a piezoelectrically driven disc with five different contrast apertures in the focal plane of the objective lens, with the sizes of 30, 70, 150, 500 and 1500 µm. The choice of contrast aperture affects the resolution and the intensity as the apertures physically block out divergent electrons. The FOCUS PEEM also has an octupole stigmator right after the contrast apertures in the back focal plane of the objective lens. This is used to correct astigmatism and non-spherical aberrations. [12]

A hexagonal iris aperture, that is continuously adjustable in size, is positioned just before the two einzel projective lenses. An einzel lens has three cylindrical tubes where the potential of the first and the last are set to equality, while the middle one has a different voltage as shown in figure 3.1 below. The beam diverges between the first two tubes, and then the beam is focused by the last two tubes, this creates a magnified image.

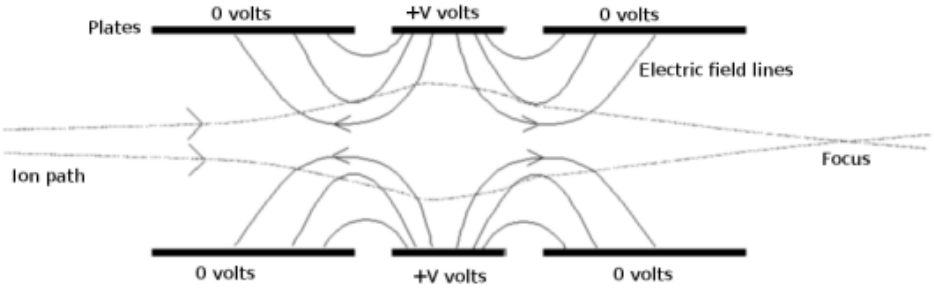

Figure 3.1 Cross section of an einzel lens. Note that the first and the last tubes do not necessarily have to be at ground potential. The beam can consist of any type of charged particle, in this image it is ions, though in the PEEM, it is always electrons. Image taken from http://en.wikipedia.org/wiki/File:Einzel_lens.png, verified 2013-06-17. Author: Wikiezz

3.3.3 Imaging Assembly

At the end of the PEEM there is a multichannel plate (MCP) that amplifies the electric signal with a factor of 10^3 - 10^5. The amplified electric signal then hits a fluorescent screen that is recorded by a CCD camera. The MCP is an expensive and fragile piece of equipment and it should always be operating at the lowest possible voltage in order to increase the life span. The noise also increases as the MCP voltage is increased. The MCP could be damaged if exposed to too high intensities. [12]

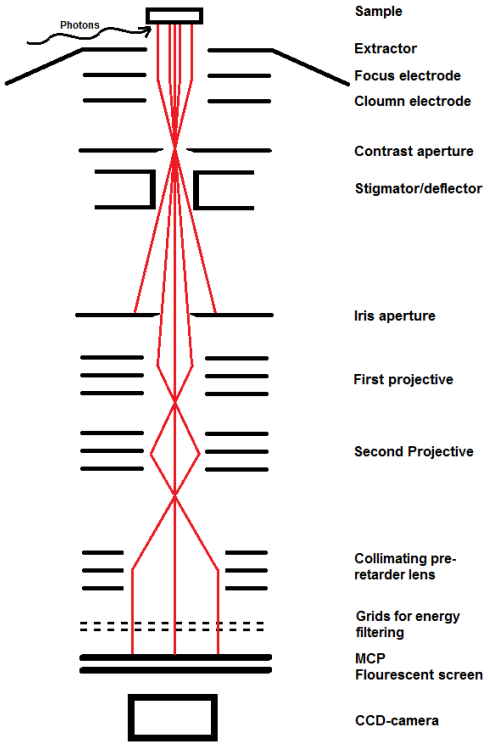

Figure 3.2 Schematic image of the interior of the PEEM with beam path. The collimating pre-retarder lens and the grids for energy filtering were never used in the experiments. Image is not to scale.

All of the three electric lenses in the PEEM do not have to be turned on. If the voltages of the projective lenses are set to the column voltage, they are turned off. The PEEM can be operated in one, two or three lens mode. In one lens mode only the objective lens is active, this is the mode with the lowest magnification. The three lens mode, when all lenses are active, has the highest magnification, but is tricky to use. [12] Two lens mode was the only mode used in the experiments because it provided enough magnification, and is quite easy to use. Furthermore, it is the only mode for which the image recorded is not upside-down, which simplifies the usage of the PEEM.

3.3.4 CCD Cameras

Two different CCD-cameras were used in the experiments. One of the cameras was a compact CCD-camera from PCO with a maximum quantum efficiency of 0.65 used for good light conditions when scanning over the sample with the Hg-lamp. [13] Real time imaging was possible with this camera, thus it suited well for scanning over the sample. The other CCD-camera was a larger camera Apogee, originally made for astronomical purposes. It had a maximum quantum efficiency of 0.86 and was used for low light conditions. Real time imaging was not possible with this camera, and thus, it was used for imaging with the laser system. The camera had a cooling system that could cool it to approximately 50^{o} C below the surrounding temperature. [14] The two cameras will from now on be referred to as the PCO and the Apogee camera for simplicity. Quantum efficiency is a notion that apprizes the amount of electrons produced per photon that hits the photoreactive surface. Quantum efficiency is wavelength dependent.

3.4 Resolution

The resolution of any type of microscope is fundamentally limited by diffraction, and so is the PEEM. The diffraction limit is inversely proportional to the wavelength of the particles that carries the information. The wavelength of the electrons in the PEEM is shorter than the wavelength of visible light, so the PEEM has a higher fundamental limit for the resolution compared to optical microscopes. This is what is unique for the PEEM, since the information carriers are electrons, optical properties of a surface can be investigated without being limited by diffraction of light. However, the diffraction limit of the PEEM has not yet been reached, instead, it is limited by other imperfections such as spherical and chromatic aberrations, space charge and astigmatism, effects that do not exist or can be greatly reduced in optical microscopes. The fundamental limit of the lateral resolution is 20 nm according to the manufacturer. [15]

3.4.1 Space charge

If the density of electrons emitted from the sample and traveling through the PEEM is too high, the coulomb repulsion can become significantly big and give rise to what is called space charge. This effect distorts the image and limits the resolution of the PEEM. [16] Small but bright objects can appear much larger than what they are because the electron cloud emitted will grow spatially and hit a larger area on the detector. An example of space charge can be found in figure 4.6. Space charge can be reduced by reducing the intensity of the incoming light, fewer electrons will then be emitted and thus there will be less prominent coulomb repulsion. However, this loss in electrons directly decreases the amount of electrons that hit the detector and thus longer exposure times are needed. The intensity should be optimized such that the space charge effect is as low as possible for the highest possible photoemission. The space charge effect is strongest in the focal plane of the lenses because the density of electrons is highest there.

3.4.2 Astigmatism and Aberrations

Astigmatism is an effect that arises when lenses are not radially symmetric or if the lenses are not positioned exactly on the optical axis. This distorts the shape of images. Astigmatism in the PEEM can be adjusted with the stigmator, using the software provided by the manufacturer. Spherical and chromatic aberration are effects that distort images and reduce resolution in an optical or electro-optical system.

In optics, spherical aberrations originate from imperfect lenses where light is bent differently at the edges compared to the center in such a way that the focal point is stretched out along the optical axis. A perfectly parabolic lens does not suffer from spherical aberration, however they are much more difficult to fabricate than spherical lenses. Electrostatic lenses suffer the same problem with spherical aberration because they are spherical, and not parabolic. The electric field is stronger at the edges than in the center, thus there will not be one single point of focus and therefore point-like objects will not be resolved as points, but as small discs.

In optics, chromatic aberration arises because the refraction index of materials depends on the wavelength of light, so different wavelengths will be focused differently. An electrostatic lens suffers from chromatic aberration as well since electrons with higher kinetic energy spend less time in the electric field of the lens. The acceleration of a particle in an electric field is proportional to the time it

spends in the field, and thus, slower electrons will be focused to a greater extent than the faster ones.

Reducing vibrations is an effort that can be made to keep the resolution as high as possible. The PEEM was lying on a heavy vibration-dampening table and an ion pump without moving parts was used to maintain UHV.

3.5 Light sources

Two different light sources were used in the experiments. The first one was a standard Hg arc-lamp supplied by Focus GmbH. The second one was a mode locked titanium-doped sapphire (Ti^{3+}:Al_2O_3) laser. It was provided by the group of Prof. Anne L'Huillier at the Division of Atomic Physics at Lund University.

3.5.1 Hg Lamp

The mercury arc lamp has a broad spectrum with a sharp peak at 4.9 eV, [17] which is above the work function of the investigated nanowires; this is crucial for the photoemission process to occur. The light from the lamp is directed onto the sample via a reflection filter that reflects UV-light, but not IR-light; this is to avoid any unnecessary heating of the sample.

3.5.2 The Laser

The linearly polarized light was generated by having the birefringent lasing crystal tilted at the Brewster angle. It was mode locked by means of a Kerr lens, capable of generating pulses as short as 5 fs. As the pulse travels through glass into the PEEM vacuum chamber, the pulse will be stretched in time since the index of refraction is wavelength dependent and the pulse has quite a large bandwidth. This was compensated for in advance by using chirped mirrors that reflect different wavelengths at different depths in the material. Wedges were placed in the beam line to adjust the amount of glass the pulse travels through, and thus the pulse length could be adjusted. However, the pulse length was never optimized. The repetition rate was adjustable from 200 kHz to 2 MHz. It was only used at 200 kHz in the experiments. The wavelength was centered on 800 nm, which implies that 3 or 4 photons were needed to knock out an electron from the sample. The laser was quite advanced and only a few of its kind exist in the world. The laser will not be further discussed as it probably requires a thesis of its own to fully explain.

4 Results

The results from the experiments will be presented in this chapter. It will contain PEEM images, SEM images and data from measurements of polarization series.

Earlier experiments have been done at the Synchrotron radiation division to investigate the photoemission of InAs nanowires and the relationship between wire orientation on the sample and the state of polarization of the light. The results seem to vary depending on wire thickness and illumination source. Therefore efforts have been made to further analyze the behavior of the nanowires when illuminated by pulsed fs laser light with a wavelength of 800 nm.

4.1 Imaging with Different States of Polarization

At first, a few nanowires illuminated by the laser are presented in figure 4.1 with the Hg image for comparison. The laser light comes in from the left in the images, while the light from the Hg-lamp comes in from the bottom.

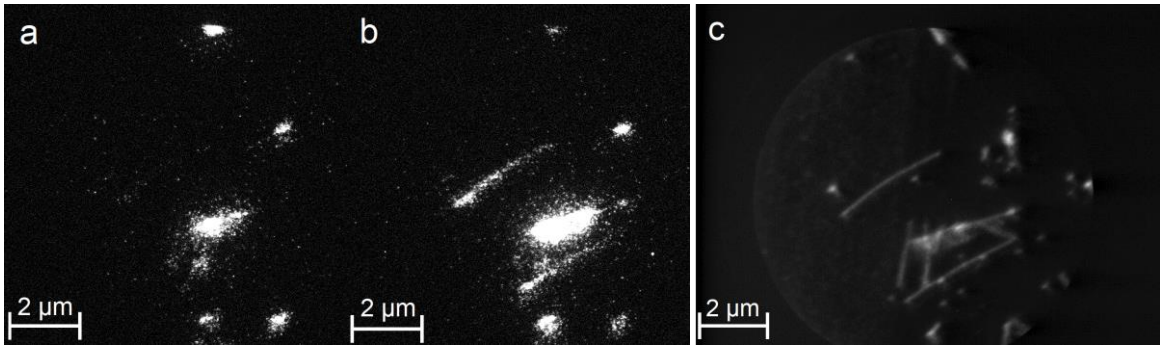

F*igure 4.1 PEEM images of some nanowires on the sample illuminated by a) S-polarized laser light, b) P-polarized laser light and c) the Hg-lamp. a and b have been rotated 90^o clockwise because the Apogee camera was rotated 90^o with respect to the PCO camera.*

One can clearly see that there is a difference in photoemission between s and p polarized light in the two images a) and b) in figure 4.1. For instance, the two wires are only visible in the second image, and seem not to respond at all to s-polarized light. Another example can be seen in figure 4.2

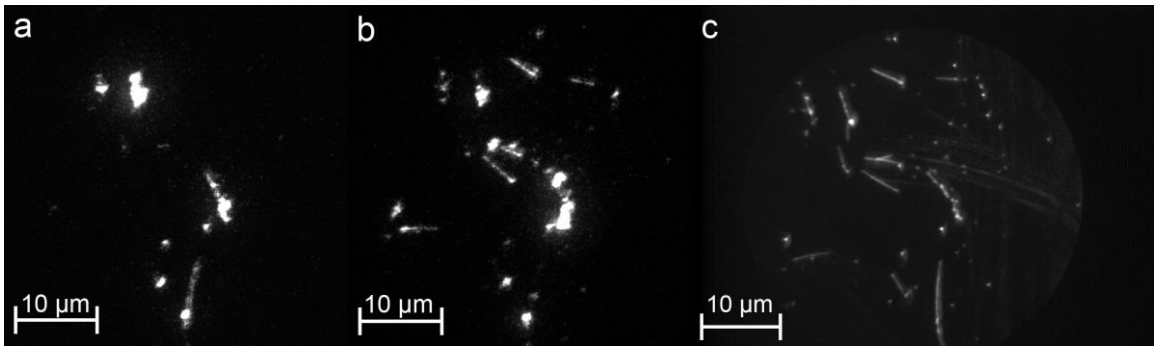

F*igure 4.2 PEEM images of some nanowires on the sample illuminated by a) S-polarized laser light, b) P-polarized laser light and c) the Hg-lamp. a and b have been rotated 90^o clockwise because the Apogee camera was rotated 90^o with respect to the PCO camera.*

Once again there is a clear difference between the photoemission of the nanowires when the state of polarization of the laser light is changed.

4.2 Clusters and Fragments of Nanowires

In the images above, one can see that the photoemission of some wires is strongly polarization dependent, while some regions seem to emit more or less the same amount of electrons regardless of the state of polarization. An explicit example of this is shown in figure 4.3 below.

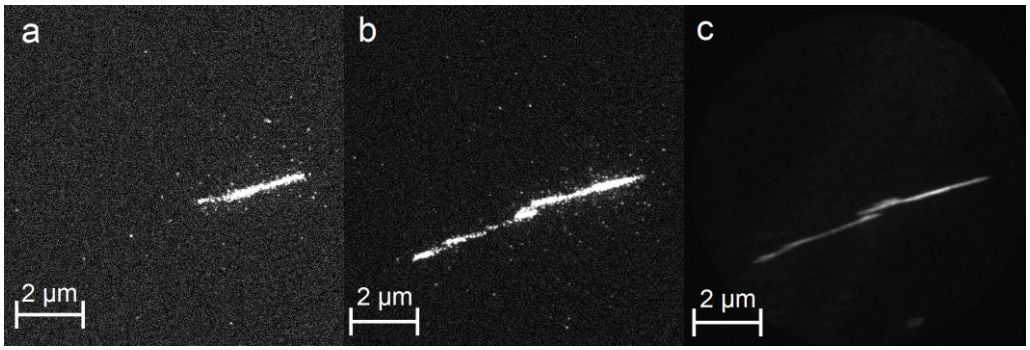

Figure 4.3 PEEM images of some nanowires on the sample illuminated by a) S-polarized laser light, b) P-polarized laser light and c) the Hg-lamp. All the images have been rotated 90^o clockwise because the Apogee camera was rotated 90^o with respect to the PCO camera.

It should be mentioned that the bright part in figure 4.3 a) does in fact drop in photoemission intensity for some angles of polarization, however it never drops to zero. This probably has to do with the fact that the bright area is not a single, nice looking wire, but a cluster of wires and fragments of wires that lie randomly on top of each other. This can clearly be seen in the SEM image, figure 4.4 below

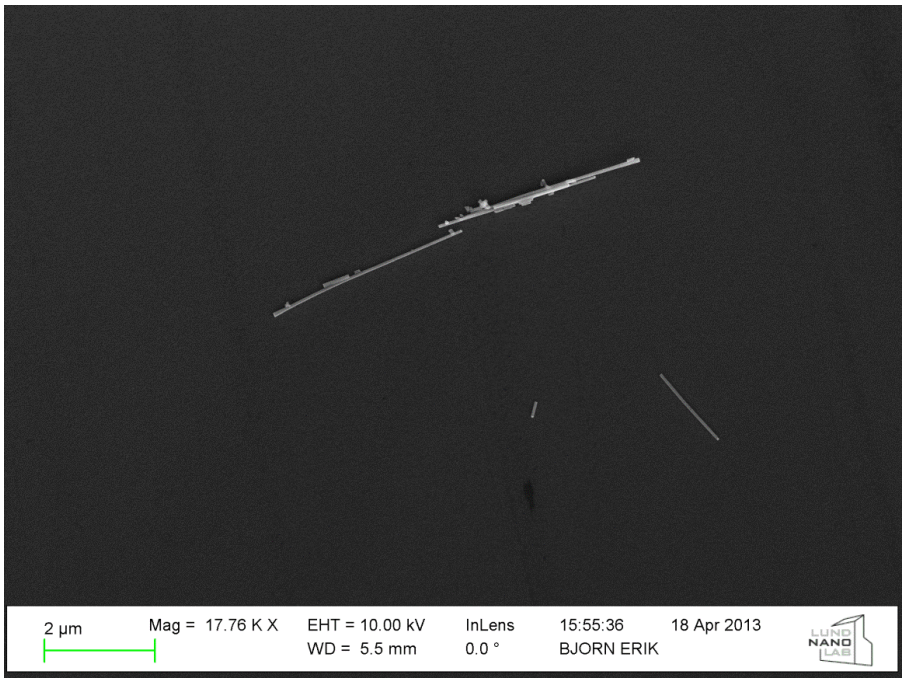

Figure 4.4 SEM image of the same are as in figure 4.3, the top wire is not a single wire but a cluster of wires and fragments of wires.

Regions like these are not included in the analysis of angular dependence because, first of all, they are hard to analyze, and second, it is more or less impossible to reproduce such a structure even if significant information could have been successfully extracted from it.

4.3 Angular Dependence

In order to investigate the angular dependence, all the analyzed wires had to be imaged with the SEM in order to verify that the wires were in fact single, nice looking nanowires and not clusters of wires. As earlier stated, the state of polarization was changed from 0^o to 360^o in steps of 10^o. All the analyzed wires will not be presented here, only a few examples.

The analysis was made using a Matlab script that Erik Mårsell had written earlier. The Matlab script measured the intensity in a selected area in the images and then the background intensity in another area. This was then used to create a polar plot of the relative intensity in the images in following way

$$\frac{I-I_{bg}}{I_{max}-I_{bg}} \tag{7}$$

where I is the intensity in the selected area and image, I_{bg} is the background intensity and I_{max} is the maximum intensity in the selected area. This yields numbers between zero and one which where plotted in polar plots. Figure 4.5 below contains such polar plots of two nanowires on the sample.

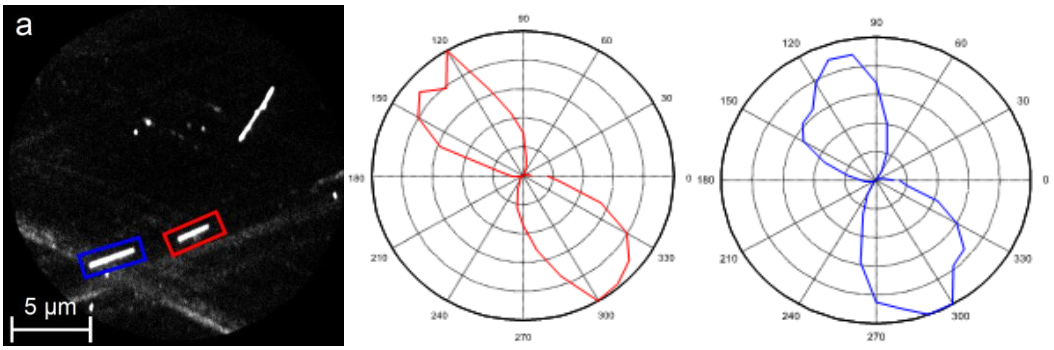

Figure 4.5 PEEM image of two straight, single nanowires with corresponding polar plots. The image is taken with the Hg-lamp. The wire enclosed in a blue rectangle corresponds to the blue polar plot and the wire enclosed in a red rectangle corresponds to the red polar plot.

From here on, the two wires in figure 4.5 will be designated the red and the blue wire, for simplicity. Figure 4.6 below illustrates the photoemission of the red and the blue wire at different angles of polarization of the illuminating laser light. Note that the nanowire in the top right corner that does not have a colored rectangle has not been measured upon since it has fragments of wires on it. A $\cos^6$ function is a good fit to the polar plots.

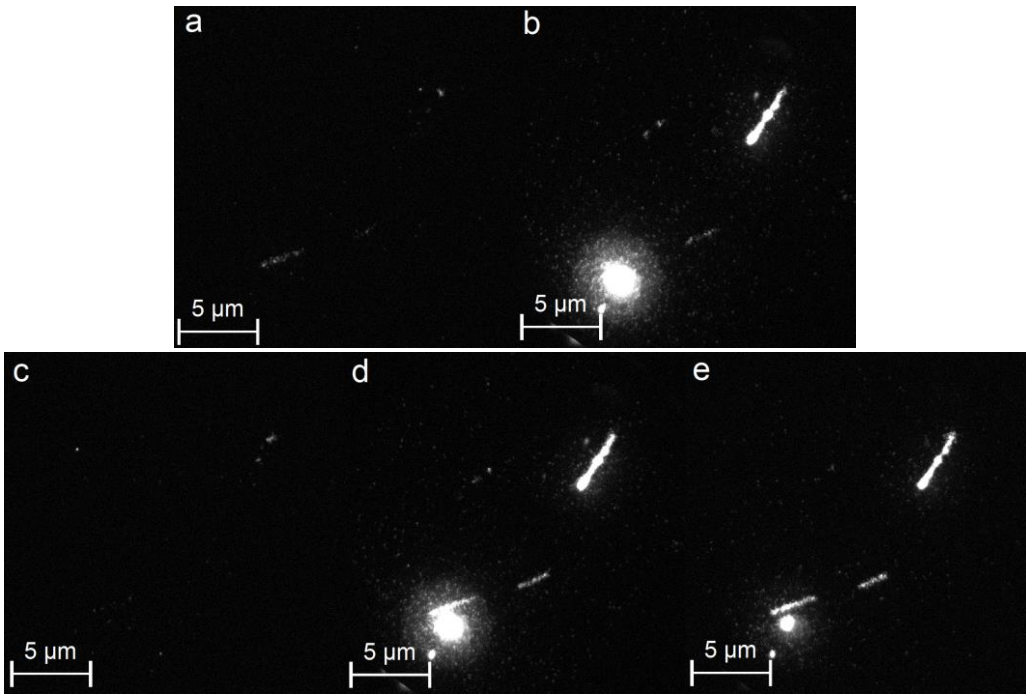

Figure 4.6 PEEM images of the same are as in figure 4.5 but illuminated with a) s-polarized laser light, b) p-polarized laser light, c) 30^o laser light that yielded minimum photoemission, d) 110^o laser light that yielded maximum photoemission for the blue wire and e) 130^o laser light that yielded maximum photoemission for the red wire.

Note the disturbing blob just below the blue wire evident in figure 4.6 b, d and e. This blob will be discussed later in section 5.3. It seems to increase and decrease in size throughout the images, due to the space charge effect.

5 Analysis

5.1 Analysis of Angular Dependence

All the clean nanowires that have been measured seemed to behave similarly to the nanowires in figure 4.5, where a $\cos^6$ function was a suitable fit for the polar plots. All the nanowires had a maximum photoemission at a certain angle of polarization. To test if this angle is related to the angle at which the wires were lying on the sample, the polarization angle of maximum emission was plotted against nanowire orientation on the sample, see figure 5.1 below. If there is a relation, the plot should yield a straight line, and if not, there should be data points at random positions all over the diagram.

The polarization angle is defined after the maximum emission angel of each wire obtained from the polar plots, where 0^o is s-polarized light and 90^o is p-polarized light. The nanowire orientation angle is defined clockwise from 0^o to 180^o as the angle of which they lie on the sample as seen from the PEEM images using the Apogee camera. A vertical wire therefore has an angle defined as 0^o while a horizontal wire is defined as 90^o. It should be mentioned that the images taken with the Apogee camera were all initially rotated 90^o counterclockwise simply because the camera was rotated with respect to the PCO camera. However in this report, the Apogee camera images have been rotated 90^o clockwise to match the images taken with the PCO camera. The result of the data analysis can be found in table 1 below. All the wires with corresponding polar plots can be found in appendix A.

Table 1 Angular data from all the nanowires measured upon.

Nanowire orientation angle [deg] The uncertainty is roughly $\pm 2^o$	Maximum emission angle [deg] The uncertainty is roughly $\pm 10^o$
150	65
170	80
60	120
70	105
68	130
50	115
50	110
90	160
100	20
108	30
57	120
130	28
110	15
90	165
140	60
90	170
90	180
10	90
40	110

The plot from the data in table 1 can be found below in figure 5.1 below.

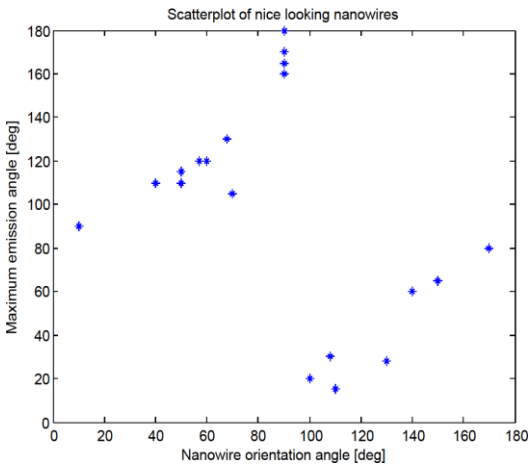

Figure 5.1 Scatter plot of nice looking wires, maximum emission angle [deg] *as a function of nanowire orientation angle* [deg]. *The nanowire orientation angle was measured quite accurately with an error of roughly ± 2^o while the polarization angle had a somewhat larger error, roughly estimated to ± 10^o.*

At first glance, this does not look very promising, however if one tries to plot it from -90^o to 90^o instead of from 0^o to 180^o, the result from figure 5.2 below is attained. The angles -90^o to 90^o are now defined as 9 o'clock to 3 o'clock respectively.

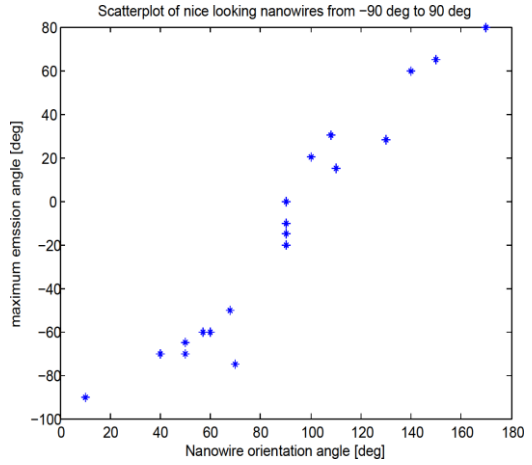

Figure 5.2 Scatter plot of the same data as in figure 5.1 but plotted from -90^o to 90^o instead of from 0^o to 180^o. -90^o is defined as 9 o' clock and 90^o is defined as 3 o' clock.

5.2 The Projection of the Electric Field

The result from figure 5.2 looks more or less like a straight line, although the data points are still quite spaced. This has to do with the fact that the incident beam is not normal to the surface of the sample, but has a grazing angle of roughly 25^o. Effectively the angle of the electric field on the sample is not the same as the angle of the electric field in the beam. The electric field vector on the sample is the projection of the electric field vector in the beam, and thus, the projection vector on the sample surface must be calculated in order to acquire a more accurate result.

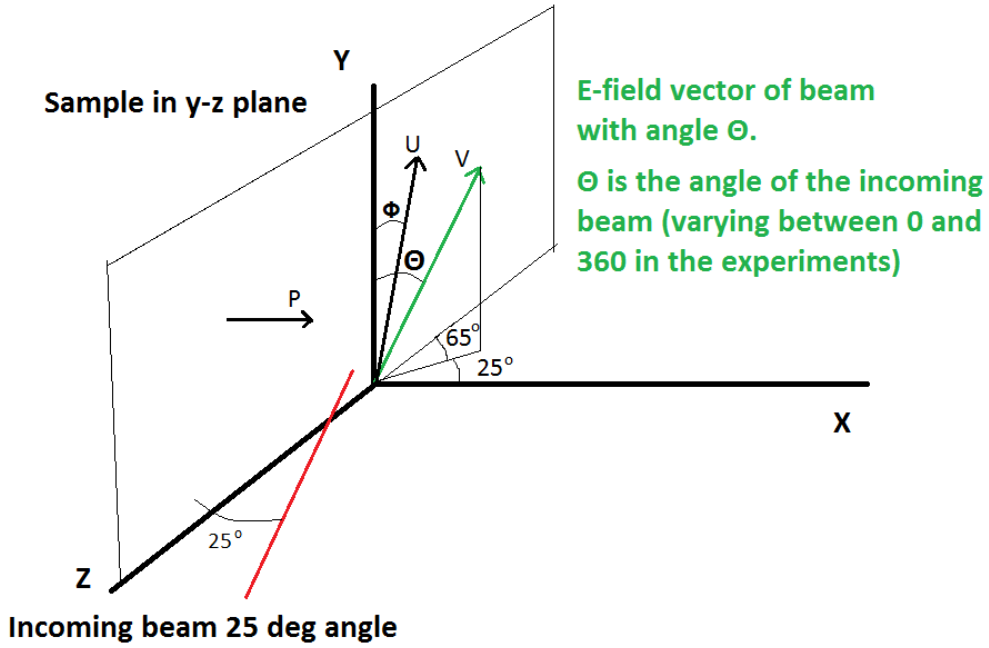

Figure 5.3 Schematic drawing of the experimental arrangement. The sample is in the y-z plane, and the emitted electrons will travel in the positive x-direction. The vector **P** *indicates the normal vector to the surface plane and the vector* **V** *indicates the electric field vector of the polarized light. Θ indicates the angle between the electric field vector and the y-axis; which varies from 0° to 360°. The illuminating laser beam comes in with a grazing angle of 25°, and thus* **V** *will rotate in the plane which is at an angle of 25° from the x-axis.* **U** *is the projection of* **V** *on the surface plane and Φ is the angle between* **U** *and the y-axis.*

In order to calculate the projection of the electric field vector onto the sample plane, the vectors **P** and **V** must first be defined. The simplest way to define the normal vector **P** is simply

$$\mathbf{P} = (x, y, z) = (1,0,0) \tag{8}$$

The vector **V** is a bit trickier but can be defined with some geometry. If the length of **V** is assumed to be unity it is easy to see that the *y*-component of the vector is simply $cos(\Theta)$, the *x*-component and the *z*-component are $cos(25°)\,sin(\Theta)$ and $sin(\Theta)\,cos(65°)$ respectively so that

$$\mathbf{V} = (cos(25°)\,sin(\Theta)\,, cos(\Theta)\,, sin(\Theta)\,cos(65°)) \tag{9}$$

To find the projection vector **U** of **V** on the surface plane the following formula was used:

$$\mathbf{U} = \mathbf{V} - (\mathbf{V} \cdot \mathbf{P})\mathbf{P} \tag{10}$$

The projection vector **U** is then

$$\begin{aligned}\mathbf{U} = {} & (cos(25°)\,sin(\Theta)\,, cos(\Theta)\,, sin(\Theta)\,cos(65°)) \\ & - (cos(25°)sin(\Theta) \cdot 1 + cos(\Theta) \cdot 0 + sin(\Theta)cos(65°) \cdot 0)(1,0,0) \\ & = (cos(25°)\,sin(\Theta)\,, cos(\Theta)\,, sin(\Theta)\,cos(65°)) - (cos(25°)\,sin(\Theta)\,, 0,0) \\ & = \big(0, cos(\Theta), sin(\Theta)cos(65)\big)\end{aligned} \tag{11}$$

so,

$$\mathbf{U} = \big(0, cos(\Theta), sin(\Theta)cos(65)\big) \tag{12}$$

Now that **U** has been calculated it is easy to see that the angle Φ is

$$\Phi = arctan\left(\frac{sin(\Theta)\cos(65°)}{cos(\Theta)}\right) \tag{13}$$

This expression can convert any angle Θ [deg] of the electric field vector **V** to the angle Φ [deg], which is the angle of the electric field on the actual surface of the sample. All the data points in figure 5.2 have to be converted from Θ to Φ using equation (13) so the correct maximum emission angle can be obtained. The converted angles can be found in table 2 below.

Table 2 The angles of the electric field vector in the beam at maximum emission converted to the angle of the electric field vector in the sample plane. The angles were converted using equation (13) above

Maximum emission angle [deg] The uncertainty is roughly ±10°	Maximum emission projection angle [deg] The uncertainty is roughly ±10°
65	42
80	67
120	-36
105	-58
130	-27
115	-42
110	-49
160	-9
20	9
30	14
120	-36
28	13
15	6
165	6
60	36
170	-4
180	0
90	-90
110	-49

The new scatter plot with the maximum emission angle in terms of Φ as a function of nanowire orientation angle is presented below in figure 5.4

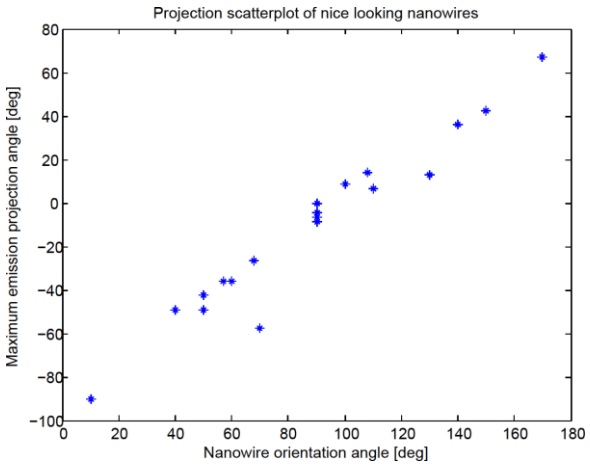

Figure 5.4 Scatter plot of nice looking wires from -90^o to 90^o. The maximum emission projection angle [deg] *as a function of nanowire orientation angle* [deg].

5.3 Bad Data Point

The graph in figure 5.4 looks much better than the graph in figure 5.2 but there is still one data point quite far off the line. In fact, this data point corresponds to the blue nanowire in figure 4.6 from before. The disturbing blob is so intense that the space charge effect causes emitted electrons to cross over the nanowire, so the measured area is contaminated with electrons from the blob. The polar plot says that the maximum emission angle of the measured area is around 105^o in terms of Θ, though the maximum emission of the actual nanowire is at a slightly different angle and because of this, the data point should be removed from the graph as in figure 5.5 below.

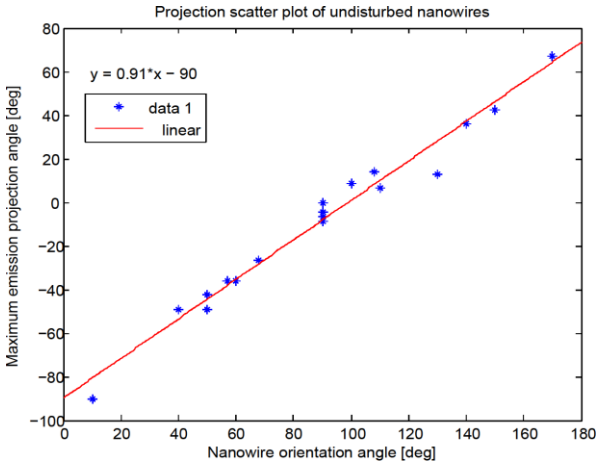

Figure 5.5 Projection scatter plot without any disturbed wires from -90^o to 90^o. The maximum emission projection angle [deg] *as a function of nanowire orientation angle* [deg]. *A linear fit was added to the graph. The equation of the linear fit is shown in the image.*

The graph in figure 5.5 indicates a clear relationship between the state of polarization on the sample and the nanowire orientation angle on the sample.

5.4 Determining the Angular Dependence

To investigate if the field enhancement is strongest when the electric field vector is parallel or perpendicular to the nanowire (or any other angle in between) a few things must be known. The PCO camera was rotated roughly 15° clockwise as viewed from the sample, the Apogee camera was then rotated 90° counterclockwise with respect to the PCO camera as seen from the sample. Figure 5.6 below presents the SEM image of the red and the blue nanowires from figure 4.5 with the orientation of the electric field on the sample that gave maximum emission. The SEM images are not rotated with respect to the images taken with the PCO camera.

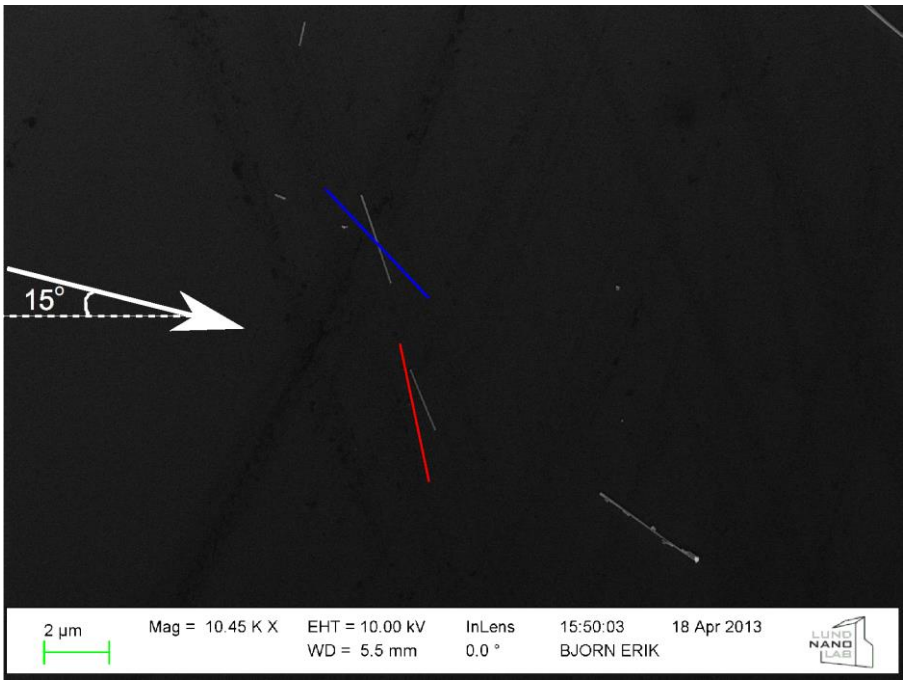

Figure 5.6 SEM image of the blue and the red nanowires from figure 4.5. The red and the blue line indicate the angle of the electric field vector that gave maximum emission for the red and the blue wire respectively. Remember that the blue wire was the wire that was removed from the scatter plot because of the disturbing fragment next to it. The white arrow represents the incoming laser beam at an angle of roughly 15° with respect to the horizontal axis in the image, the same angle at which the PCO camera was rotated with respect to the sample.

The maximum emission angle in terms of Θ for the red wire in figure 5.6 above was 110° which converts to -26.7° in terms of Φ. But because the 15° rotation of the CCD camera with respect to the sample, the resulting electric field angle in the image will be $-26.7° + 15° = -11.7°$. The red line is drawn at this angle and it overlaps quite will with the red nanowire next to it. The same procedure has been done for the blue line, and because of the disturbing fragment, the overlap is not quite as good as for the red wire.

5.5 Analysis of Data from 2012

Earlier experiments that have been conducted with the same type of sample but with a different laser system have not acquired the same results as in this thesis. The sample that had previously been studied was not the exact same sample as studied in this thesis, but it was nanowires taken from the same batch and put on a piece of wafer that was cut from the same wafer. Thus, there

should be no reason to distinguish between the two samples. The result from an earlier experiment is shown below in figure 5.7.

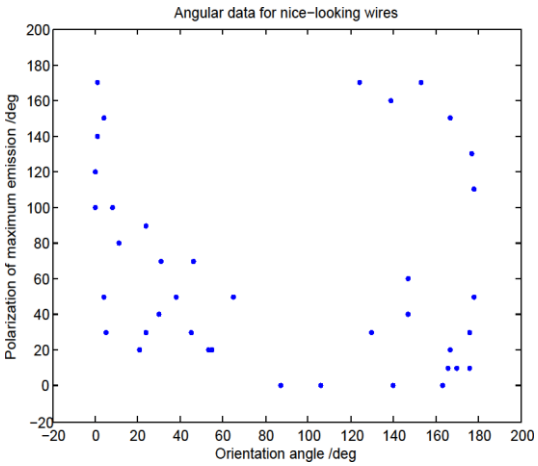

Figure 5.7 Data from 2012 of the same type of wires as in this thesis but with a different laser system. Plot of the polarization angle in the laser beam as a function of nanowire orientation angle. There seems to be no relation between the angle of polarization and the nanowire orientation angle.

The results of measurements from 2012 shown in figure 5.6 do not at all resemble the result of the measurements from 2013. Because of this, the data from 2012 were double checked by carefully analyzing it again. To do this, all the raw data from 2012 was analyzed without looking at the previous analysis, thus getting rid of any bias. Only straight, single nanowires were selected and analyzed in the same way as had been done with the data from 2013. The result is shown in figure 5.8 below.

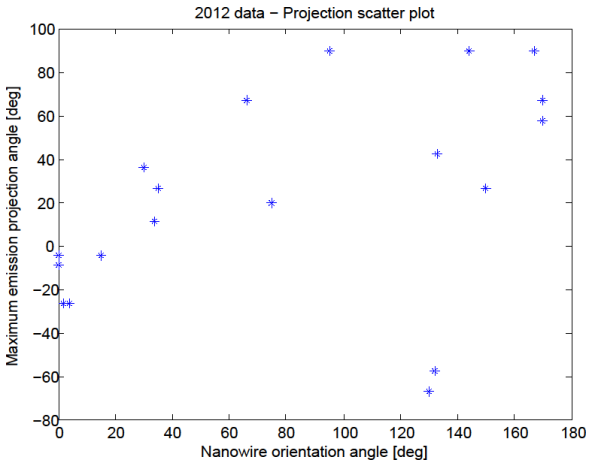

Figure 5.8 Data from 2012 reanalyzed without bias and with carefully chosen nanowires. Plot of the maximum emission projection angle as a function of nanowire orientation angle.

Figure 5.8 shows that there are some wires with almost the same angle of which they lie on the sample, but with completely different angles of maximum emission.

6 Conclusion and Discussion

6.1 Discussing the Data

There is a clear difference between the data from 2012 and 2013 even though the samples were the same; the only difference between the measurements were the laser systems. It is reasonable to believe that the differences in the laser systems cause the differences in the measurements. The repetition rate of the laser used in 2012 was 1 kHz, while 200 kHz for the laser used in this thesis. Having a higher repetition rate is beneficial for the resolution since a higher average intensity can be acquired for the same maximum intensity, thus reducing the space charge effect. Although a higher resolution was convenient, especially when doing the measurements in Matlab, it should not alone cause the big differences. The spectra of the two lasers were not exactly the same either, and maybe most importantly the intensities were different. Even relatively small differences between the lasers could potentially imply large differences in the measurements as the lasers significantly affect the nanowires. Too high intensities and repetition rates could for instance melt the nanowires.

Another noteworthy difference was that some wires from the 2012 measurements did not seem to respond at all to the laser. The wires were clearly visible with the Hg lamp and in the SEM, but did not show up at all when illuminated by the laser. Generally speaking, the data from 2012 was much more ambiguous, some wires did not show up at all, some wires only emitted electrons at a certain point and it was much harder to determine what was what in the images. An example of this is shown in figure 6.1 below.

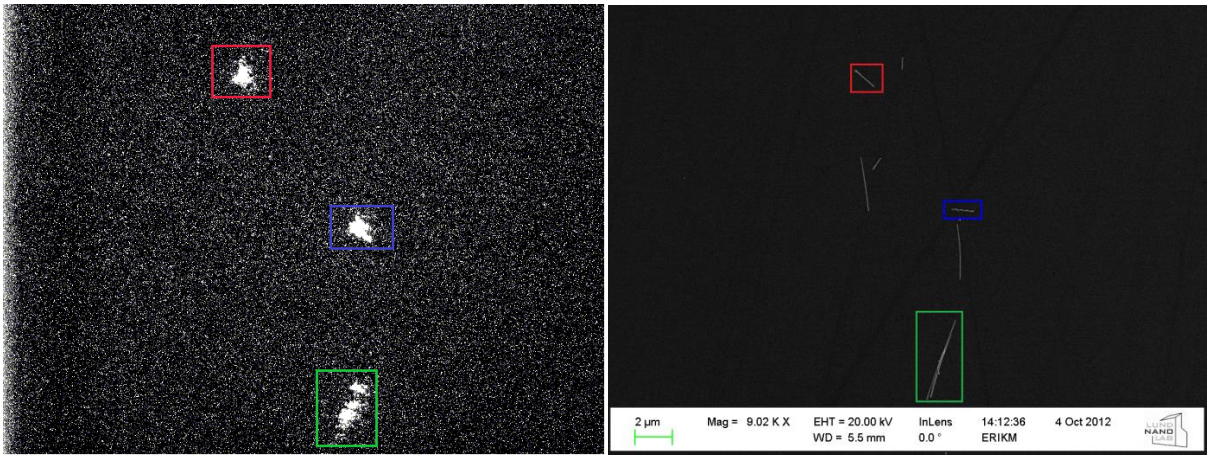

Figure 6.1 Images of nanowires taken 2012. The left image is taken when the sample was illuminated with p-polarized laser light and the right image is the SEM image of the same nanowires. The colored rectangles indicate the wires that are visible in the left image. The wires that are not visible in the left image are not visible for any of the other angles of polarization either.

If the left image in figure 6.1 is compared with for instance figure 4.1 one can clearly see a difference in resolution. In figure 4.1 the wires are clear, while in figure 6.1 the visible nanowires barely resemble wires at all. The wires respond differently to different states of polarization. Therefore it is not strange that the wires do not show up in the images for some states of polarization. However, the wires in figure 6.1 that are not visible in the left image do not show up at all for any state of polarization.

Examining the graph in figure 5.5, the linear curve has a slope of 0.91. The curve is expected to be periodical around 180^{o} since there is no reason to distinguish between a wire orientated at 0^{o} and 180^{o}. Since 0.91 is fairly close to 1, which is periodic, the results are quite trustworthy. The slope of 0.91 instead of 1 probably arises from experimental inaccuracies. If the linear curve would have had a slope of for instance 0.5 or 2, which is quite far from periodic, the results would not have been as reliable.

It is important to mention that not only straight, single nanowires show a dipole behavior in the polar graphs. Almost any nanostructure, even clusters of wires tend to have a clear dipole behavior. This probably has to with the fact that MPPE is a non-linear process. The photoemission is, according to perturbation theory, proportional to the intensity to the power of 2 for double-photon photoemission (2PPE) and 3 for tripple-photon photoemission (3PPE) etc. This is an approximation from perturbation theory that does not hold for MPPE when the number of transitions becomes too many. This, together with the fact that the intensity is proportional to the electric field squared, has serious implications on the photoemission. If the field enhancement for one resonance is twice as strong as for another, the photoemission will be 2^{6} = 64 times larger. This means that the weaker resonance will not be seen at all.

For straight, single nanowires, the strongest resonance seems to be along the wire (according to 2013 measurements), however this does not necessarily have to be the case for clusters of wires. In a single nanowire, it is reasonable to think that light can couple most efficiently to the nanowire when the electric field is along the wire, much like in a polarizer. However, in a cluster of wires, the situation is not so simple and the strongest resonance can be orientated in any direction.

6.2 Correcting for Missing Angles

As seen earlier, the angle of the electric field in the beam is not the same as in the plane of the sample. Not only were the angles different, but while the angle in the beam was changed equidistantly, the angle in the sample plane was not. The angle of the electric field in the sample did not change linearly with respect to the angle in the beam. This can be seen in table 3 and figure 6.2 below.

Table 3 Angles of the electric field vector in the laser beam and in the sample plane

Angle of electric field vector in the beam [deg]	Angle of the projection of the electric field vector onto the sample plane [deg]
0	0
10	4,3
20	8,7
30	13,7
40	19,5
50	26,7
60	36,2
70	49,3
80	67,4
90	±90
100	-4,3
110	-8,7
120	-13,7
130	-19,5
140	-26,7
150	-36,2
160	-49,3
170	-67,4
180	±90

The angles of the second column in table 3 above are drawn in figure 6.2 below.

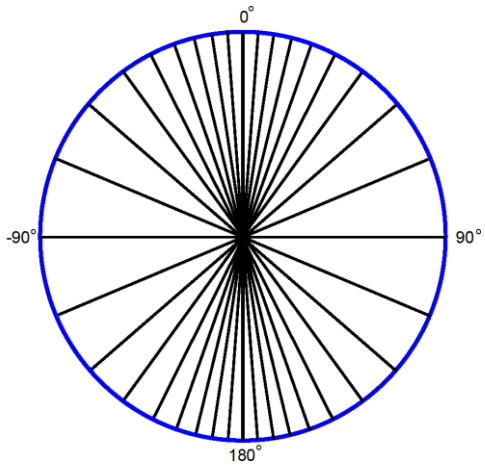

Figure 6.2 The black lines in the circle represent the orientation of the electric field vector in the plane of the sample. The angles on the circle correspond to the angles in table 3 above. Note that there is a larger gap between the lines when the angle approaches 90°.

Looking at figure 6.2, one can see that the spacing between the data points increases as the angle approaches 90°, decreasing the accuracy of the measurements around those angles. In future experiments of this kind, a few more data points should be added near 90°.

6.3 XUV Chamber and Future Experiments

So far, the samples have been studied with the PEEM and the SEM only to investigate the optical properties of the samples, and frankly to see what the samples look like. In the future, the idea is to do time resolved experiments with a pump probe laser setup to study field enhancements in the form of plasmonics. Although an extensive theory of plasmonics will be left aside, a few words should be mentioned to elucidate the connection between the subject of plasmonics and the future experiments.

A plasmon is a charge density wave in the electron gas. This collective motion of electrons is not a real particle in itself, but is said to be a quasi-particle. If a plasmon is confined to the surface of a conductor or a semi-conductor, it is called a surface plasmon and if the surface plasomon is propagating, it is called a surface plasmon polarition (SPP). These SPPs can be generated by photons and then guided along nanowires. [18] It is unlikely to generate so called plasmons in semi-conductors with light at optical frequencies; plasmonic resonances require quite high charge densities, as can be found in metals and therefore plasmonic resonances are usually studied in metallic nanostructures. The subject of plasmonics is applied to many different fields of technology, one of which is computer technology. Compared to the electronics in circuit boards, fiber optics is capable of transmitting a large amount of information in a short period of time, however the bulky nature of the wires are a limiting factor. The idea is to merge these two together through plasmonics, to get the speed and performance of optics, and the miniature size of the electronics. Nanowires could thus be used to guide optical signals on the circuit boards in a computer.

In future experiments, the pulsed IR-laser is proposed to be the pump laser which generates surface plasmons on the sample, with a high harmonic generated (HHG) extreme ultraviolet laser (XUV) pulse as the probe. This allows for time resolved experiments that enables the investigation of the behavior of the surface plasmons. As the IR pulse hits the sample, it can spawn a surface plasmon, the XUV pulse then comes in at a time slightly later than the IR pulse and effectively "takes an image" of the surface plasmon. This is done a couple of hundred thousand times per second since the repetition rate is in the 200 kHz-2 MHz regime. One pulse of light is not enough since it only releases a hand full of electrons. Sufficient intensities are reached by means of many pulses. The screen recorded by a CCD-camera will look like a still image with all of these hundreds of thousands of "images" on top of each other. An image of the screen can be taken. The XUV pulse is then delayed to come in ever so slightly later than before to take "images" of the plasmons at later times in their "lives", and a new image of the screen can be captured. Repeating this process yields many different images at different times in the surface plasmons lives and these images could be put together in order to create a video.

Since XUV light is extremely interactive, it is heavily absorbed in glass, and therefore cannot be transmitted into the vacuum chamber through a glass window. The HHG of the XUV pulses must take place inside the vacuum chamber itself. This requires a few modifications of the vacuum chamber since it must be connected to the HHG vacuum chamber. The XUV pulse cannot be focused by means of normal optical lenses. Instead a multicoated mirror designed for XUV light is used. The advantage of this is that chromatic aberrations do not exist in mirrors. Even though spherical aberrations are still present, the mirror is designed to diminish these when it sits at a grazing angle of 12^{o}.

7 References

[1] Richard Feynman. *QED - The Strange Theory of Light and Matter*, p. 85, 20-21 (1985)

[2] Christopher J. Foot. *Atomic Physics*, p. 125 (2005)

[3] Harrison Benson, *University Physics*, revised Edition, p. 841 (1996)

[4] B. Gilbert, R. Andres, P. Perfetti, G. Margaritondo, G. Rempfer, G. De Stasio, *Compensation of charging in X-PEEM: a successful test on mineral inclusions in 4.4 Ga old zircon*, Ultramicroscopy, **83,** p.129 (2000)

[5] John F. O'Hanlon, *A users guide to vacuum technology*, third edition. p. 183-185, 201-202, 210, 213, 255-260 (2003)

[6] Yanovsky, V. et al. Opt. Express, **16**, 2109-2114 (2008)

[7] B. E. A Saleh, M. C. Teich, *Fundamentals of Photonics*, second edition. p. 543-545, 546, 548, 618-619, 620

[8] T. D. Donnelly and C. H .Grossman, *Ultrafast Phenomena: A Laboratory Experience for Undergraduates,* Am. J. Phys. **66**, 677 (1998).

[9] AvA. E. Siegman, *Lasers*, p. 334 (1986)

[10] Wagner, R.S and W.C. Ellis, *Vapor-Liquid-Solid mechanism of Single Crystal Growth.* Appl. Phys. Lett. **4**, 89 (1964)

[11] Daniel Jacobsson, *Crystal structure determination of III-V nanowires,* Licentiate Thesis, p. 10-13

[12] Focus GmbH, Omicron NanoTechnology. *Instruction Manual Focus PEEM*, version 2.2 (2007)

[13] PCO, http://www.pco.de/categories/sensitive-cameras/pcopixelfly-usb/, verified 2013-06-17.

[14] Apogee Imaging Systems, http://www.ccd.com/alta_f32.html, verified 2013-06-17

[15] Omicron NanoTechnology GmbH. http://www.omicron.de/en/products/focus-peem-/instrument-concept, verified 2013-06-17

[16] N. M. Buckanie, J. Göhre, P. Zhou, D. von der Linde, M. Horn-von Hoegen and F-J Meyer zu Heringdorf, *Space charge effects in photoemission electron microscopy using amplified laser pulses*, J. Phys: Condens. Matter **21** (2009)

[17] Focus GmbH, Omicron NanoTechnology. *Instruction Manual Hg Arc UV source*, version 2.0 (2005)

[18] Y. Fang et. al. *Branched silver nanowires as controllable plasmon routers,* Nano letters, **10**, p. 1950-1954 (2010)

Appendix A - SEM Images with Corresponding Polar Plots

All the nanowires from 2013 that have been analyzed are presented in this appendix. The colored rectangles around the wires do not necessarily indicate the measured area around a wire, but indicates which wire corresponds to which polar plot.

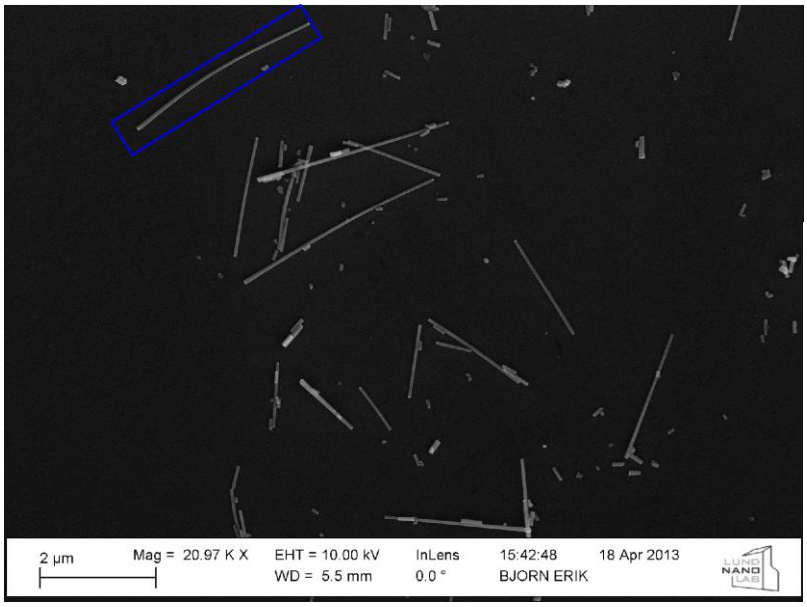

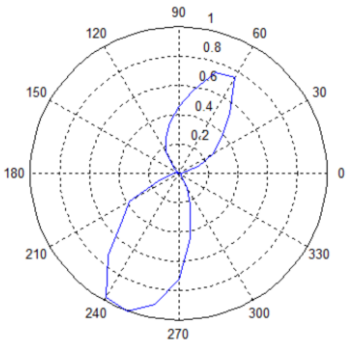

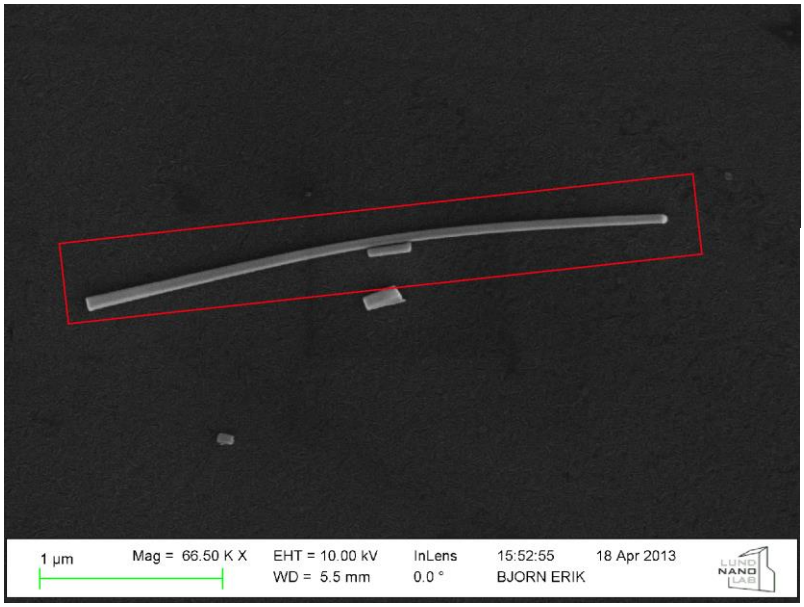

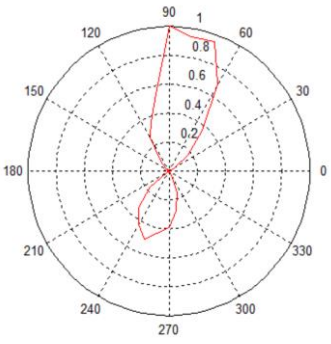

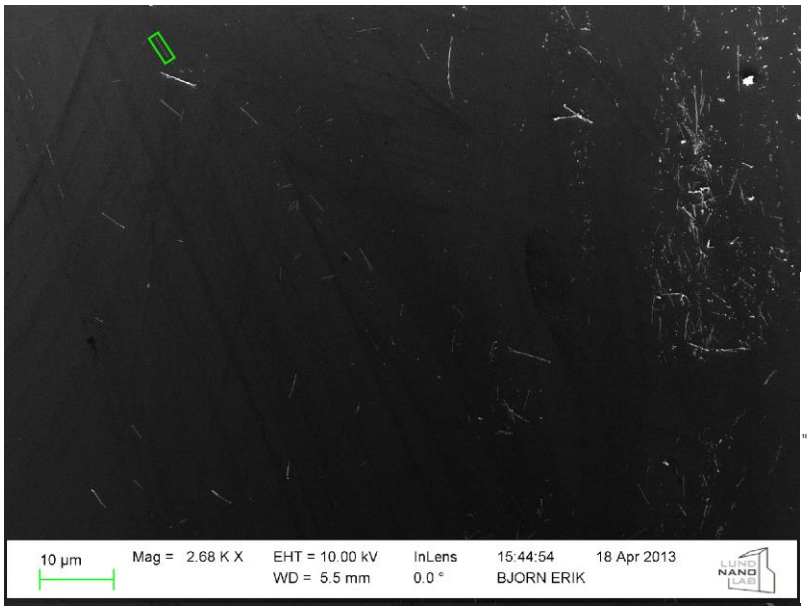
10 µm
Mag = 2.68 K X
EHT = 10.00 kV
WD = 5.5 mm
InLens
0.0 °
15:44:54
BJORN ERIK
18 Apr 2013

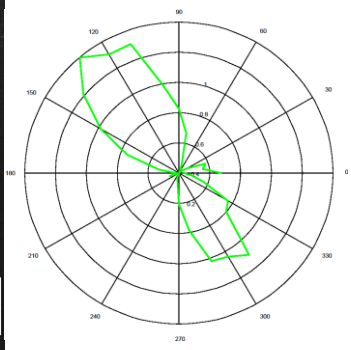

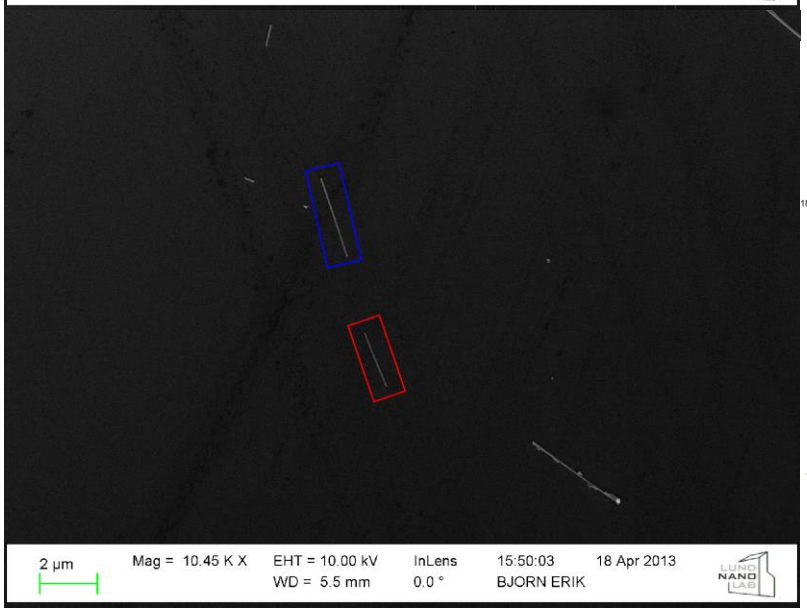
2 µm
Mag = 10.45 K X
EHT = 10.00 kV
WD = 5.5 mm
InLens
0.0 °
15:50:03
BJORN ERIK
18 Apr 2013

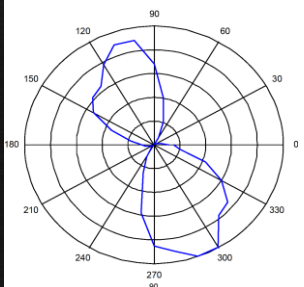

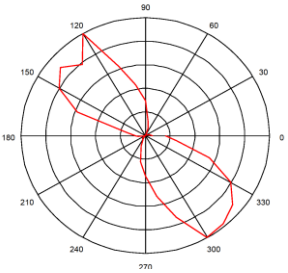

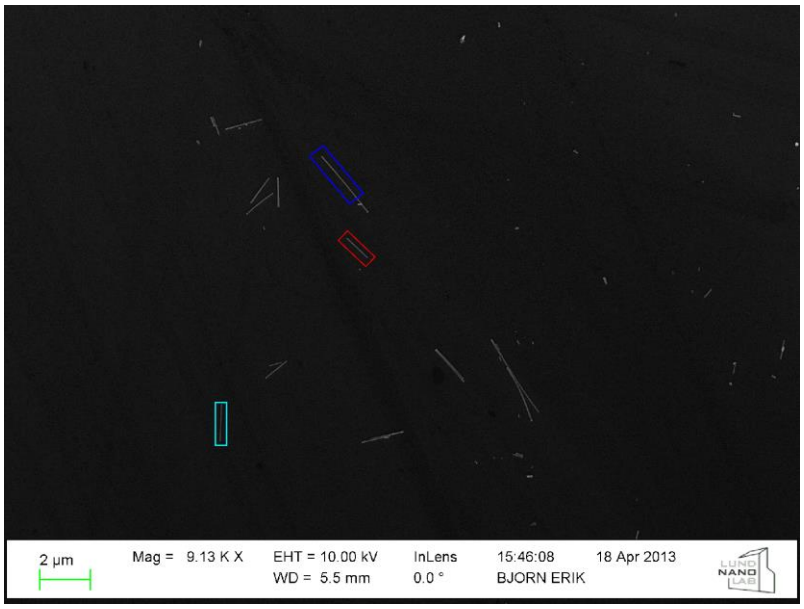
2 µm
Mag = 9.13 K X
EHT = 10.00 kV
WD = 5.5 mm
InLens
0.0 °
15:46:08
BJORN ERIK
18 Apr 2013

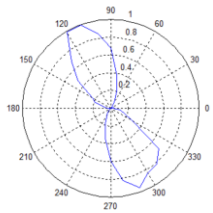

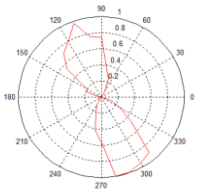

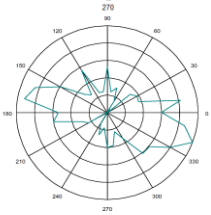

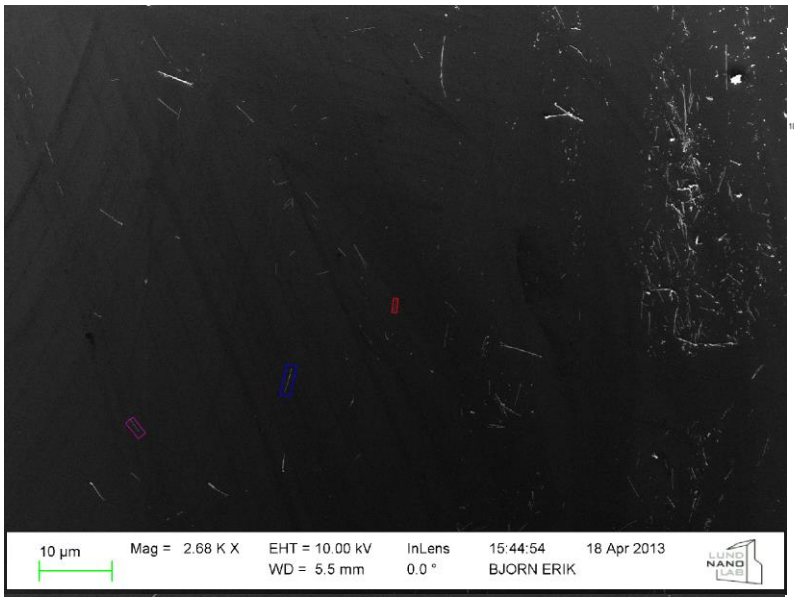
10 µm
Mag = 2.68 K X
EHT = 10.00 kV
WD = 5.5 mm
InLens
0.0 °
15:44:54
BJORN ERIK
18 Apr 2013

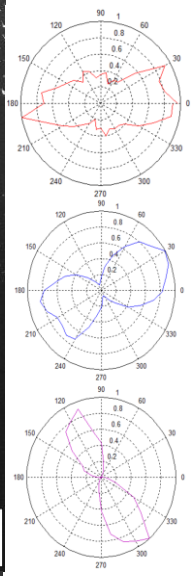

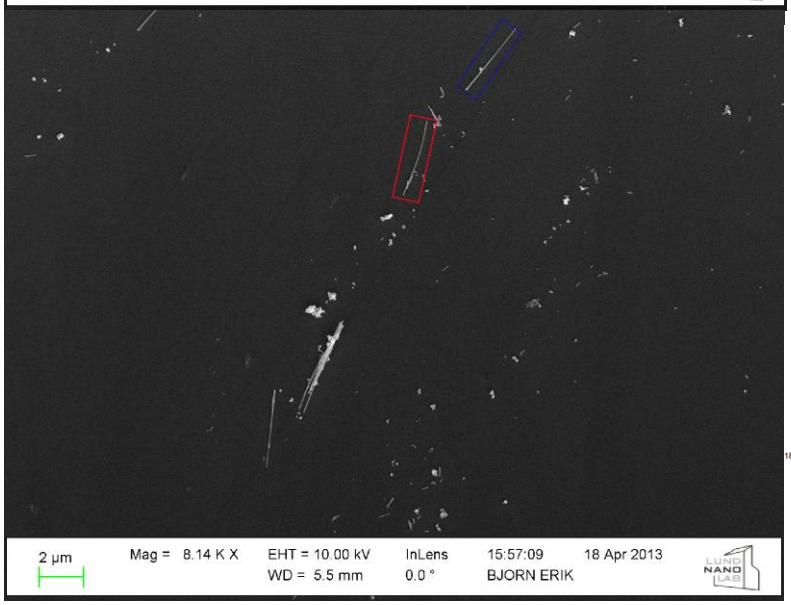
2 µm
Mag = 8.14 K X
EHT = 10.00 kV
WD = 5.5 mm
InLens
0.0 °
15:57:09
BJORN ERIK
18 Apr 2013

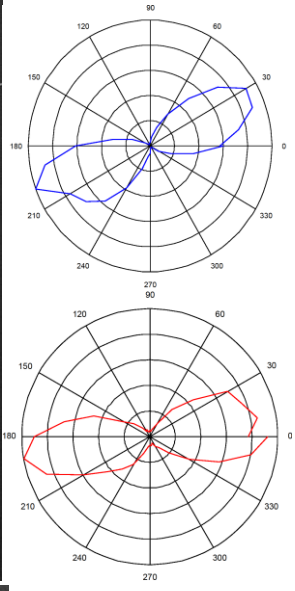

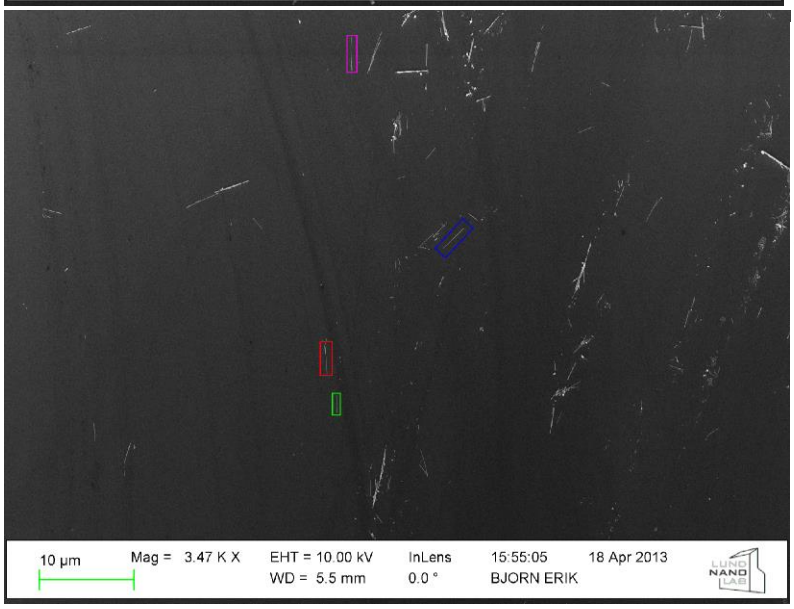
10 µm
Mag = 3.47 K X
EHT = 10.00 kV
WD = 5.5 mm
InLens
0.0 °
15:55:05
BJORN ERIK
18 Apr 2013

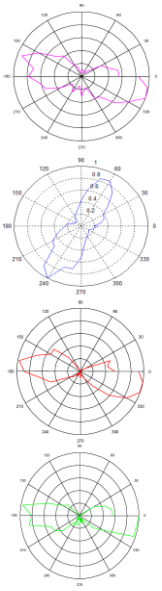

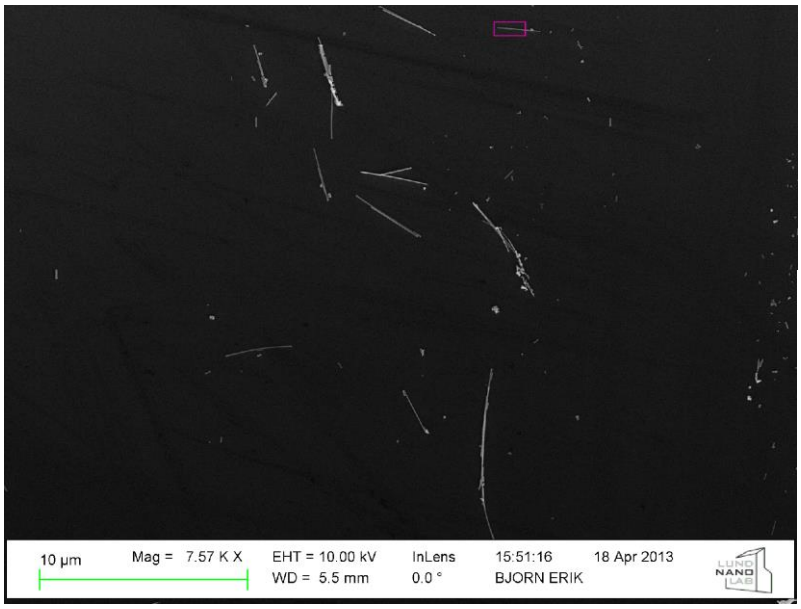
10 µm
Mag = 7.57 K X
EHT = 10.00 kV
WD = 5.5 mm
InLens
0.0 °
15:51:16
BJORN ERIK
18 Apr 2013

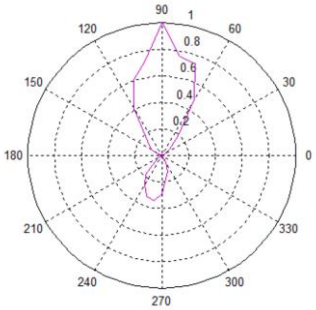
90
1
120
60
0.8
0.6
150
30
0.4
0.2
180
0
210
330
240
300
270


2 µm
Mag = 17.76 K X
EHT = 10.00 kV
WD = 5.5 mm
InLens
0.0 °
15:55:36
BJORN ERIK
18 Apr 2013

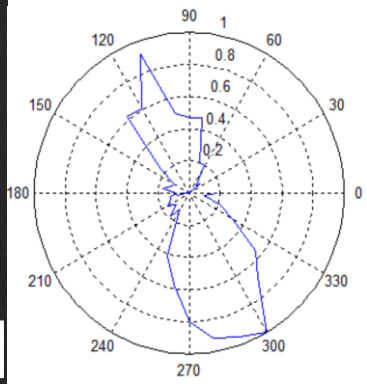
90
1
120
60
0.8
0.6
150
30
0.4
0.2
180
0
210
330
240
300
270